The final publication is available doi: 10.2967/jnumed.112.110700

Site-specific radiometal labeling and improved biodistribution using ABY-027, a novel HER2-targeting affibody molecule-ABD fusion protein

Anna Orlova[1§*], Andreas Jonsson[2§], Daniel Rosik[2§], Hans Lundqvist[3], Malin Lindborg[4], Lars Abrahmsen[4#], Caroline Ekblad[4], Fredrik Y. Frejd[3,4], Vladimir Tolmachev[3§]

1 Preclinical PET Platform, Medicinal Chemistry, Uppsala University, Sweden;

2 School of Biotechnology, Division of Molecular Biotechnology, Royal Institute of Technology, Stockholm, Sweden;

3 Division of Biomedical Radiation Sciences, Rudbeck Laboratory, Uppsala University, Uppsala, Sweden;

4 Affibody AB, Solna, Sweden;

§ Former affiliation: Affibody AB, Solna, Sweden.

Present affiliation: Algeta ASA, Oslo, Norway.

* Corresponding author: Anna Orlova, anna.orlova@pet.medchem.uu.se,

Fax: +46(0)18 471 5307, Phone: +46(0)73 9922 846,

Dag Hammarskjöldsv 14C, 3 tr, 751 83 Uppsala, Sweden.

Financial support: This work was supported by grants from Swedish Research Council (Vetenskapsrådet) and Swedish Cancer Society (Cancerfonden).

Disclosures:

Affibody AB holds intellectual property rights and trademarks for Affibody molecules, which might be considered as a potential conflict of interest. However, we believe that we have presented data and considerations in a scientifically strict and unbiased way and refer to results published in established international peer-review journals.

ABSTRACT

Due to better penetration, smaller targeting proteins may be superior to antibodies for radioimmunotherapy of solid tumors. Therefore, affibody molecules (6.5 kDa) have a potential for being suitable as targeted moiety for radiolabeled therapeutic proteins. Previous studies have demonstrated that a fusion of an affibody molecule with an albumin-binding domain (ABD) provides a strong non-covalent binding to albumin in vivo. This can be used for reduction of the renal uptake of the affibody molecule while maintaining a size smaller than that of an antibody, which is important when using residualizing radionuclide labels conjugated to affibody molecules. The goal of this study was to design and evaluate a new targeting affibody-ABD fusion protein with improved biodistribution properties for radionuclide therapy.

Methods. A novel affibody-based construct, $Z_{HER2:2891}$-ABD_{035}-DOTA (ABY-027), was created by fusion of the re-engineered HER2-binding affibody molecule $Z_{HER2:2891}$ to the N-terminus of the high-affinity ABD_{035}, and a maleimido-derivative of DOTA was conjugated at the C-terminus of the construct. Binding and processing of ^{177}Lu-ABY-027 by HER2-expressing cells were evaluated in vitro. Targeting of HER2-expressing SKOV-3 xenografts was evaluated in BALB/C nu/nu mice and compared with targeting of previously reported ABD-$(Z_{HER2:342})_2$.

Results. The binding affinity (dissociation constant) of ABY-027 to HER2 (74 pM) was the same as for the parental $Z_{HER2:2891}$ (76 pM). ABY-027 was stably labeled with ^{177}Lu and ^{111}In with preserved specific binding to HER2-expressing cells in vitro. In vivo receptor saturation experiments demonstrated that targeting of SKOV-3 xenografts in BALB/C nu/nu mice was HER2 specific. ^{177}Lu-ABY-027 demonstrated substantially (2-3 fold) lower renal and hepatic uptake in comparison with previously assessed HER2-specific affibody-based albumin-binding

agents. Tumor uptake of radiolabeled ABY-027 at 48 h pi was 2-fold higher than that for previously reported ABD-$(Z_{HER2:342})_2$.

Conclusions. An optimized molecular design of an ABD-fusion protein resulted in an affibody molecule construct with better properties for therapy. Fully preserved in vivo targeting of the fusion protein was shown in xenografted mice. Site-specific coupling of DOTA provides a uniform conjugate and creates potential for labeling with a broad range of therapeutic radionuclides. The biodistribution of ^{177}Lu-ABY-027 in a murine model suggests it is more suitable for therapy than alternative approaches.

Key words: HER2, affibody molecule, lutetium-177, targeting therapy, albumin

INTRODUCTION

During the last decades, an impressive progress in the treatment of disseminated cancer has been achieved. Conventional chemotherapy has been supplemented with new therapeutic modalities that exploit the recognition of unique molecular features of cancer cells or the microenvironment in tumor tissue. This has resulted in increased selectivity of several therapies and reduced toxicity to healthy tissues. One cancer-associated molecular target for therapy is the human epidermal growth factor receptor type 2 (HER2, Neu, ErbB2). HER2 is a member of the epidermal growth factors tyrosine kinase receptor family involved in regulation of cell proliferation, motility and apoptosis suppression. HER2 is overexpressed in many types of carcinomas and is considered to be part of the malignant phenotype (*1*). A recent review reports HER2 overexpression frequency of 25% for breast cancer, 20-70% for hormone-refractory prostate cancers, and 35-55% for colorectal cancer (*1*). In contrast, HER2 expression in normal adult tissues is very low or non-detectable. Treatment of HER2-expressing breast cancer with trastuzumab, a HER2-specific antibody, significantly prolongs survival of breast cancer patients (*2*). Unfortunately, many HER2-expressing breast cancers have primary resistance and others develop treatment-induced resistance to the HER2-binding monoclonal antibody trastuzumab within one year (*3*). Resistance often develops despite sustained HER2 expression (*3*).

The persistence of HER2 expression may be utilized for targeting a payload to the tumor cells, including cytotoxic agents and radionuclides (for a recent review see (*4*)). Radionuclide therapy offers the advantage of a cross-fire effect occurring when nuclides delivered to cancer cells irradiate neighboring malignant cells. This can overcome issues associated with heterogeneous expression of a particular malignant target or non-uniform penetration of targeting agents into the tumor tissue (*5*). Radioimmunotherapy of non-Hodgkin lymphoma using the radiolabeled antibodies ^{131}I-tositumomab and ^{90}Y-ibritumomab tiuxetan has demonstrated high response rates and constitutes an encouraging example of targeted radionuclide therapy (*6*). However, targeted

radionuclide therapy of solid tumors using immunoglobulins remains a challenge (*7*). The major reasons are the long residence time of the large (150 kDa) immunoglobulins in circulation, resulting in irradiation of healthy tissues, such as bone marrow, and slow extravasation and penetration into the tumor limiting the therapeutic effect (*8*). The slow diffusion and poor penetration of antibodies into solid tumors has raised interest in smaller targeting proteins as carriers for radionuclides and other payloads. Proteins with a mass below the cut-off for renal clearance (around 60 kDa) are rapidly lost from the blood stream (*9*). Despite the short circulatory half-life high affinity proteins may yield high levels of solid tumor targeting, probably because of greatly superior tumor penetration, as exemplified with a 6.5 kDa HER2 binding affibody molecule (*10,11*).

Our approach is to make targeted therapeutic agents based on affibody molecules. Affibody molecules constitute a new class of affinity proteins based on a 58-amino acid residue protein domain derived from staphylococcal protein A (for recent reviews see (*12,13*)). Affibody molecules combine small size (~6.5 kDa) with high affinity and specificity for the target. Most studied is the $Z_{HER2:342}$ affibody molecule, binding to HER2 with high affinity, K_D 22 pM (*11*). Clinical utility for imaging of HER2-expression in patients with metastasized breast cancer was demonstrated using a ^{111}In- and ^{68}Ga-labeled chemically manufactured variant of $Z_{HER2:342}$ (*14*). The main obstacle for using affibody molecules with residualizing radiometal labels for radionuclide therapy is their predominant renal excretion associated with nearly quantitative tubular re-absorption (*15-17*). The renal concentration of radioactivity in a murine model at 4 h after injection was as high as 250% ID/g for affibody variants labeled with ^{111}In or ^{177}Lu using a DOTA chelator (*15,16*).

One of the approaches for the generation of the new targeting agents is to assemble the targeting molecule from smaller parts providing the desired biological and pharmacological properties. In our previous studies (*17,18*), we demonstrated that fusion of the anti-HER2 affibody molecule dimer $(Z_{HER2:342})_2$ to a 5 kDa, non-cysteine-containing, three-helix bundle albumin binding

domain (ABD), modified the pharmacokinetics. The residence time in blood was appreciably extended and the renal uptake was reduced 20-30-fold in comparison with non-ABD-fused affibody molecules. The ^{177}Lu-CHX-A''-DTPA-ABD-($Z_{HER2:342}$)$_2$ conjugate demonstrated curative effect in murine microxenografts with high HER2 expression (*17*). In a parallel study Dennis et al., showed that a fusion protein of a Fab-fragment and an albumin-binding peptide is superior to the Fab fragment in terms of tumor penetration (*19*). Serum albumin has previously been shown to preferentially locate in tumors compared to normal tissue (*20*), and the favorable tumor penetration of an albumin associated fusion protein might be a result of combining favorable localisation with high affinity binding to a protein on the tumor cell surface.

In the present study the improved HER2 targeted affibody molecule $Z_{HER2:2891}$, has been combined with an engineered ABD fusion protein ABD_{035}, having a very high affinity (K_D 50-500 fM) for human serum albumin (*21*). ABD_{035} also displays higher affinity for murine serum albumin compared to the parent ABD, found in the HER2-binding fusion protein used in our previous study. The affibody molecule $Z_{HER2:2891}$ is an engineered derivative of $Z_{HER2:342}$ used in that study. The target binding surface has been retained but the non-binding surface has been optimized and is distinctly different compared to the parental molecule (*22*). $Z_{HER2:2891}$ was recently validated in a clinical trial and was shown to target HER2-expressing metastatic lesions in breast cancer patients (*23*). In the novel fusion protein, denoted ABY-027, the affibody moiety was inserted N-terminally of the ABD, to separate the HER2 and the albumin binding surfaces as far as possible: in the affibody molecule the HER2 binding surface is located on helices 1 and 2, whereas in the ABD the albumin-binding surface it is located on helices 2 and 3 of the triple helical protein domain. Last, the chelating group used for labeling the fusion protein was site-specifically introduced, utilizing a unique cysteine residue specifically introduced for this purpose.

The goal of this study was to evaluate the biodistribution and targeting properties of the new potential anti-HER2 therapeutic agent $Z_{HER2:2891}$-ABD_{035}-C-DOTA (further denoted ABY-027).

MATERIALS AND METHODS

General.

^{177}Lu-lutetium and ^{111}In chloride were from Covidien (Netherlands). Buffers used for conjugation and labelling were purified from metal contaminations using a Chelex 100 resin (Bio-Rad Laboratories). The NAP-5 size exclusion columns were from GE Healthcare (Uppsala, Sweden). The radioactivity was measured using an automated gamma-counter with a 3-inch NaI(Tl) detector (1480 WIZARD, Wallac Oy). The radioactivity distribution on the ITLC strips was measured by a Cyclone™ Storage Phosphor System and analyzed using the OptiQuant™ image analysis software. CHX-A''-DTPA-ABD-$(Z_{HER2:342})_2$ was produced and labeled with indium-111 as described earlier (*14*,*15*).

Production of $Z_{HER2:2891}$-ABD_{035}-DOTA (ABY-027)

A DNA-fragment encoding $Z_{HER2:2891}$ (*22*) was sub-cloned into a pET (Novagen) derived expression vector containing a gene encoding ABD_{035} (*21*) with a C-terminal cysteine, resulting in the expression vector pAY02107. Soluble protein was produced in *E. coli* and purified using HSA-Sepharose (CNBr-activatied Sepharose™ 4FF, Amersham Biosciences AB) as described earlier (*17*). The $Z_{HER2:2891}$-ABD_{035} was conjugated to maleimide-DOTA (Macrocyclics) as described by Ahlgren (*24*). The conjugate was analyzed by high-performance liquid chromatography and online mass spectrometry (HPLC-MS) using an Agilent 1100 HPLC/MSD equipped with Zorbax 300SB-C18 (4.6 × 150, 3.5 μm) column. Binding kinetics and affinity of ABY-027 for HER2-Fc chimera and for human serum albumin (HSA) was measured using a Biacore 2000 instrument (GE Healthcare) according to methods described earlier (*21*,*22*).

Labeling Chemistry

For labeling, an aliquot of 50 µg ABY-027 in 0.5 M sodium acetate containing 10 mg/mL ascorbic acid, pH 5.5, was mixed with a pre-determined amount (65-76 MBq) of ^{177}Lu or ^{111}In and incubated at 60 or 80^{o}C for 30 minutes. A metal-to-ligand ratio of 1:5 was used for labeling. For routine quality control of the labeling, ITLC SG (silica gel impregnated glass fiber sheets for instant thin layer chromatography, Gelman Sciences Inc.) was used, eluting with 0.2 M citric acid.

For a stability test, two aliquots of ^{177}Lu-ABY-027 were mixed with a 500-fold molar excess of EDTA, incubated for 60 min at ambient temperature and analysed as described above. Amount of non-protein-bound ^{177}Lu was compared with a standard, not exposed to EDTA.

In vitro Studies

The HER2 expressing ovarian carcinoma cell line SKOV-3 (ATCC, LGC Standards AB, Boras, Sweden), displaying approximately 1.6x10^{6} HER2 receptors per cell (*25*), was used in this study. All experiments were performed in triplicate.

The binding specificity for HER2-expressing cells of the ^{177}Lu-ABY-027 conjugates labeled at 60 or 80°C was tested using methods described earlier (*17*). For HER2-blocking, a 1000-fold excess of non-labeled affibody molecule was used. Cells were incubated with labeled conjugate (0.5 nM) for 1 h at 37°C and the percentage of cell-bound radioactivity was determined in blocked and non-blocked samples.

The antigen binding capacity of ^{177}Lu-ABY-027 labeled at 60°C or 80°C was determined using methods described earlier (*17*). A solution of ^{177}Lu-ABY-027 in cell culture medium (1 ml, 0.06 pmol) was added to cell pellets to provide approximately 100-fold molar excess of receptor over

conjugate. The cells were incubated for 5 h at 4˚C and the percentage of cell-bound radioactivity was determined.

Cellular retention and processing of ^{177}Lu-ABY-027 by HER2 expressing cells was studied according to the method described earlier (*26*). Cells were incubated with radiolabeled affibody conjugate (5 nM) for 1 h at 4°C. The media was then exchanged and incubation was continued at 37°C. The membrane-associated radioactivity was determined at pre-selected time-points. The percentage of small (<5 kDa) radiocatabolites in the incubation media was determined by analysis using NAP-5 size-exclusion columns.

In vivo Studies

The animal studies were approved by the Local Ethics Committee for Animal Research. The tumor was grafted by subcutaneous (s.c.) injection of ~10^7 SKOV-3 cells in hind legs of female Balb/c nu/nu mice. Tumors were allowed to grow for 4-5 weeks before experiments. In all biodistribution studies groups of 4-6 animals were used. At pre-determined time points, the animals were euthanized by heart puncture under anesthesia (Ketalar, 10 mg/ml; Rompun, 1 mg/ml, 20 µl of solution per gram body weight). Blood and organ samples were excised and weighed, and their radioactivity was measured. The tissue uptake values were calculated as percent injected dose per gram tissue (% ID/g).

For comparison two group of mice were injected with 50 kBq ^{111}In-ABY-027 (10 µg) and ^{111}In-CHX-A'' DTPA-ABD-$(Z_{HER2:342})_2$ (16 µg) in 100 µl PBS, and biodistribution was measured at 48 h after injection. An average tumor weight was 0.2±0.1 g.

To evaluate the influence of the injected ABY-027 protein dose on tumor uptake and biodistribution of ^{177}Lu-ABY-027, three groups of mice were injected with 20 kBq in 100 µL PBS per mouse. The protein dose was adjusted to 1, 10, or 50 µg per mouse by mixing with non-

labeled ABY-027. The biodistribution was compared at 48 h after injection. An average tumor weight was 0.14±0.07 g.

In order to evaluate the biodistribution and tumor targeting capacity of the labeled compound, and to obtain input data for dosimetry calculations, 24 mice were injected with 120 kBq ^{177}Lu-ABY-027 (protein dose 10 µg in 100 µL PBS) each. An average tumor weight was 0.10±0.05 g. At predetermined time points (4, 24, 48, 72, 168 and 336 h p.i.) a group of four mice was euthanized, and concentration of the radioactivity in tumors and tissues was determined. To confirm HER2-specific tumor targeting of ^{177}Lu-ABY-027, four mice were injected with 1 mg each of non-labeled ABY-027. One hour later, the mice were injected with 120 kBq ^{177}Lu-ABY-027 (protein dose 10 µg in 100 µL PBS) each. The animals were euthanized 48 h after injection, and biodistribution of radioactivity was determined.

Dosimetry Calculations

The dosimetry calculations were performed according to methods described earlier (*17*). Briefly, the organ uptake values from the biodistribution study, noncorrected for physical half-life, were time integrated by the trapezoid method to obtain the residence time per gram tissue. The extrapolated area was less than a few percent in all organs. In the absorbed dose calculations, S values for ^{177}Lu were obtained from RADAR phantoms (Unit Density Spheres) ((http://www.doseinfo-radar.com/) The S value for a 1 g sphere (0.0233 mGy/MBq s) was used generally to calculate all organ doses. This simplified dosimetry calculation is motivated by the fact that the low-energy β-particles in the ^{177}Lu decay are locally absorbed, and photons and other penetrating radiations are contributing to a low extent, which means that the cross-talk between different organs in the mouse is negligible.

Statistics

Statistical analyses were performed by un-paired, two-tailed *t*-test using Prism (version 4.00; GraphPad Software) for Windows (Microsoft). *P* value below 0.05 was considered significant.

RESULTS

Characterization of $Z_{HER2:2891}$-ABD_{035}-DOTA (ABY-027)

The identity and purity of $Z_{HER2:2891}$-ABD_{035}–cys and $Z_{HER2:2891}$-ABD_{035}-DOTA were characterized by HPLC-MS and SDS PAGE. Both analyses confirmed the expected mass of the constructs (12122 and 12646 Da respectively). The purity of $Z_{HER2:2891}$-ABD_{035}-DOTA was above 98%, as determined by HPLC-MS. No other variants than 1:1, chelator to protein ratio was detected. Binding kinetics of ABY-027 to the extracellular domain of HER2 was measured using surface plasmon resonance. The association rate constant (k_a) was $(8.78\pm0.06)\times10^6$ $M^{-1}s^{-1}$, the dissociation rate constant (k_d) was $(6.45\pm0.03)\times10^{-4}$ s^{-1}, and the dissociation constant (K_D=kd/ka) was 74 pM. Retained high albumin binding affinity was confirmed, and shown to be similar to that of the single domain ABD_{035} used as control. Due to the very high affinity, it was not possible to determine the exact dissociation constant using surface plasmon resonance

Labeling Chemistry

The labeling of ABY-027 was rapid and efficient under the selected conditions. Labeling with ^{177}Lu at 60^{o}C provided yields of 94±7% after 15 min and 98±2% after 30 min (n=6). At 80^{o}C, the yields were 96±3%, and 97±1% after 15 and 30 min, respectively. The specific radioactivity was 1.3-1.5 MBq/µg (16.4-19.3 GBq/µmol) depending on the specific radioactivity of ^{177}Lu-lutetium chloride. Challenge with 500-fold molar excess of EDTA during 1 h did not reveal any measurable release of radioactivity. Labeling yields were 98.8% for ^{111}In-ABY-027 and 99.1% for ^{111}In-CHX-A''-DTPA-ABD-$(Z_{HER2:342})_2$.

Cellular Binding and Retention

Binding of ^{177}Lu-ABY-027, labeled at 60°C or 80°C, was significantly decreased by pre-incubation with an excess of non-labeled compound that demonstrated receptor mediated binding (Figure 1).The binding competent fraction of ^{177}Lu-ABY-027 labeled at 60°C during 30 min was 88±1%. Increasing the labeling temperature up to 80°C significantly decreased the binding competent fraction to 81±2% (p=0.02). As labeling at 80^{o}C did not provide higher yield or more rapid labeling, further biological experiments were performed with conjugates labeled at 60^{o}C.

Cellular retention and processing experiment demonstrated good retention of ^{177}Lu radioactivity after interrupted incubation of SKOV-3 cells with ^{177}Lu-ABY-027 (Figure 2A): Half of the cell-associated radioactivity was retained at 24 h after interrupted incubation. Most of the radioactivity release occurred during the first four hours. Only half of the cell-associated radioactivity had been internalized after 24 h. A size exclusion chromatography of incubation medium showed that after 24 h incubation approximately 40% of the radioactivity in the medium was associated to low-molecular weight (<5 kDa) radiocatabolites, indicating that a part of the conjugate was processed intracellularly and radiocatabolites excreted (Figure 2B).

Tumor Uptake and Biodistribution

Direct comparison of biodistribution pattern of ^{111}In-ABY-027 and ^{111}In-CHX-A''-DTPA-ABD-$(Z_{HER2:342})_2$ in tumor bearing mice (Table 1) demonstrated 2-fold higher tumor uptake and 3-fold lower radioactivity retention in kidneys for ^{111}In-ABY-027. Radioactivity concentration in other studied tissues was slightly higher for ^{111}In-ABY-027. Data for ^{111}In-CHX-A''-DTPA-ABD-$(Z_{HER2:342})_2$ were in good agreement with published results (*17*,*18*).

Data on the influence of ABY-027 protein dose on tumor uptake and biodistribution of ^{177}Lu-ABY-027 in mice bearing SKOV-3 xenografts are presented in Figure 3. No dose-dependent

significant difference in organ accumulation of radioactivity at 48 hours after injection of 1, 10 or 50 µg of ABY-027 can be seen, except from a slightly (but significantly) higher retention of radioactivity in the carcass in mice injected with 1 µg conjugate. The apparent lower tumor concentration of ^{177}Lu in mice injected with 50 µg of conjugate, was not significantly separate from the value obtained with 10 µg ($p > 0.05$). In further experiments, a dose of 10 µg per animal was used.

Data on the biodistribution of ^{177}Lu-ABY-027 in Balb/C nu/nu mice bearing SKOV-3 xenografts at different time points after injection are presented in Figure 4 and Table 2. The mean tumor weight was 98±42 mg in these experiments. Figure 4 presents the results of the targeting specificity test. The tumor radioactivity concentration at 48 h after injection was decreased from 17±7 to 5±1%ID/g ($p<0.015$) by pre-injection of 1 mg of non-labeled ABY-027. There was no significant difference in the radioactivity concentrations in all other organs and tissue samples. The decrease of ^{177}Lu-ABY-027 uptake in the tumor by pre-saturation of HER2 confirms that the tumor-targeting is receptor-mediated.

^{177}Lu-ABY-027 demonstrated efficient targeting of HER2-expressing SKOV-3 xenografts in nude mice (Table 2). Already at 24 h after injection, the tumor radioactivity concentration was equal to the radioactivity concentration in blood and higher than in all other studied organs and tissue samples. The concentration of ^{177}Lu in tumors peaked at 48 h after injection followed by slow wash-out. Up to 14 days after injection, the concentration of the radioactivity in the tumor exceeded the concentrations in any other organs. The blood clearance was slow with an elimination half-life of 41 h. The concentration of radioactivity in excretory organs (kidneys and liver) was lower than in tumors and blood, peaking between 24 and 48 h after injection.

Dosimetry Calculations

The fraction of decays per gram of the administered activity (the residence time) was calculated by integrating the kinetic data (AUC) obtained in BALB/c nu/nu mice bearing SKOV-3 tumor xenografts and is presented in Table 3. The contribution of extrapolated data was small, less than 10%. The residence time was multiplied with a conversion factor to obtain the absorbed dose given in Table 3. The data on a previous ABD-fused affibody molecule variant, ^{177}Lu-CHX-A''-DTPA-ABD-$(Z_{HER2:342})_2$ (*14*), are provided for comparison. The data were obtained in the same xenograft model and calculated using the same method. The comparison suggests that the ratio of doses to tumor and bone is equal for both conjugates. At the same time, tumor-to-liver (4.9 for ^{177}Lu-ABY-027 vs 2.8 for ^{177}Lu-CHX-A''-DTPA-ABD-$(Z_{HER2:342})_2$) and tumor-to-kidney (3.9 for ^{177}Lu-ABY-027 vs 1.4 for ^{177}Lu-CHX-A''-DTPA-ABD-$(Z_{HER2:342})_2$) dose ratios were appreciably higher for ^{177}Lu-ABY-027.

DISCUSSION

Targeted delivery of cytotoxic radionuclides is one potential option for treatment of HER2-expressing malignant tumors that are resistant to receptor blocking therapies. Numerous attempts have been made with smaller proteins having better extravasation and penetration in tumors than antibodies. However, several studies have demonstrated that the use of small HER2-targeting proteins such as $(Fab')_2$ (*27*), diabodies (*28*), DARPins (*29*), nanobodies (*30*) and affibody molecules (*16,24*) labeled with radiometals all resulted in a high concentration of radioactivity in the kidneys. In each case, the renal concentration of radioactivity exceeded the tumor concentration several fold, suggesting a high risk of severe nephrotoxicity as a side-effect of targeted radionuclide therapy.

We have previously shown that fusion of a dimeric anti-HER2 affibody molecule with an albumin-binding domain provided a protein capable of strong binding to albumin in vivo (*17,18*). This prevented rapid glomerular filtration and tubular re-absorption, and endowed a conjugate

with favorable targeting properties for radiotherapy. Dosimetry calculations demonstrated that the dose to the tumor exceeded the dose to the kidney 1.4-fold, and curative treatment in a microxenograft model was possible (*17*). However, a further reduction of renal uptake would be desirable and the present study was based on the hypothesis that a stronger binding to albumin might reduce the renal uptake of the radiolabeled conjugate. Furthermore, a strong binding to albumin is also expected to minimize losses due to lysosomal catabolism following pinocytosis of albumin carrying the conjugate, by enabling maximal utilization of neonatal Fc receptor mediated salvage of albumin (*31*). Thus ABD_{035} with femtomolar affinity for albumin may offer a pharmacokinetic advantage as a fusion partner to new targeting agents.

The surface plasmon resonance experiment showed that ABY-027 binds to HER2 with an affinity (K_D=74 pM) identical to the affinity of parental $Z_{HER2:2891}$ (K_D=76 pM). This supported our assumption that the HER2-targeting moiety should preferably be situated at the N-terminus of the fusion protein to preserve the affinity by minimizing sterical interference from ABD. The construct was efficiently and stably labeled with ^{177}Lu at 60^{o}C with preserved HER2 binding capacity (Figure 1). The cellular processing experiment suggested moderate internalization rate (Figure 2), however more rapid than that for the parent anti-HER2 affibody molecule (*24*).

As expected a clear effect on the half-life of ABD binding to the serum albumin was demonstrated. The elimination half-life of the parental $Z_{HER2:2891}$ affibody molecule from blood was increased 80-fold, from 0.5 h (*24*) to 41 h. Furthermore, biodistribution experiments with ABY-027 labeled with luthetium-177 in SKOV-3 xenografted mice showed more than 3-fold reduced renal accumulation of radioactivity in comparison with ^{177}Lu-CHX-A''-DTPA-ABD-$(Z_{HER2:342})_2$ (*17*), with retained tumor uptake. Targeting of HER2-expressing xenografts was specific, as saturation of HER2 by pre-injection of an excess non-labeled ABY-027 caused a significant decrease of tumor uptake (Figure 4). At the same time, targeting was equally efficient in a broad range of injected protein doses (Figure 3). Thus, ^{111}In-ABY-027 provides an efficient

expansion of the plasma half-life and a reduction of renal uptake of affibody molecules, as well as specific and improved targeting of HER2-expressing xenografts in comparison with previously reported ABD-$(Z_{HER2:342})_2$ (Table 1). Importantly, the circulatory half-life of ^{177}Lu-ABY-027 in mice was 2-2.5-fold shorter than the half-life of radiolabeled anti-HER2 antibodies (*25*,*32*) and the molecular weight of ^{177}Lu-ABY-027-albumin adduct (ca. 80 kDa) is approximately half the weight of an antibody. This should reduce problems seen when using antibodies for radioimmunotherapy, such as too long residence time in blood and poor tumor penetration. It has been previously shown that the penetration of an Fab-albumin-binding peptide:albumin complex (size approximately 120 kDa) was much better than what would be assumed from its size and at least equal to that of the non-complexed Fab (*19*). We have previously shown a curative effect of targeted radionuclide therapy in mice carrying SKOV-3 xenografts using an anti-HER2 affibody molecule fused with the first generation ABD (*17*), in contrast to the mAb pertuzumab only yielding prolonged survival in the same tumor model (*25*).

As discussed above, the current affibody ABD fusion protein is a development from the first generation HER2-binding ABD fusion protein (*17*,*18*). Recently, Hoppman and co-workers (*33*) evaluated the alternative approach of direct chemical coupling of $Z_{HER2:342}$ to human serum albumin (HSA). We have made a comparison of the biodistribution of these different constructs, using the data from 48 hours after injection as this was the only common time point (Table 1). The study of the construct ^{111}In-DOTA-ABD-$(Z_{HER2:342})_2$ was done in mice xenografted with the low-HER2-expressing cell line LS174T, which may explain the lower tumor values compared to the other three constructs studied in xenografts of the high-HER2-expressing cell line SKOV-3. Furthermore, also xenografts based on the same cell line may show batch to batch variability as well as variable in biodistribution pattern of the same conjugate labeled with different radionuclides (*34*). Therefore comparisons are preferably done head-to-head in the same batch of xenografts, as with ^{111}In-ABY-027 and ^{111}In-CHX-A''-DTPA-ABD-$(Z_{HER2:342})_2$ in the present

study. However, data from normal tissues should be directly comparable. Despite multiple HER2-binding, the HSA-conjugate did not provide the highest tumor accumulation compared to the fusion proteins analyzed in the high-HER2-expressing xenograft model. Furthermore, the high levels in liver and spleen, as well as the faster clearance, suggest negative effects of multiple random conjugations on the properties of albumin. On the contrary, the novel fusion protein based on affinity matured ABD provided the lowest kidney values, and also the lowest values in liver and spleen. A comparison of dosimetry of ^{177}Lu-ABY-027 and ^{177}Lu-CHX-A''-DTPA-ABD-$(Z_{HER2:342})_2$ (*17*) are presented in Table 3. Both calculations were based on the same methodology and the biodistribution input data were obtained in the same animal model, Balb/C nu/nu mice bearing SKOV-3 xenografts. A curative effect was obtained after injection of 21.6 MBq ^{177}Lu-CHX-A''-DTPA-ABD-$(Z_{HER2:342})_2$, (*17*). With ^{177}Lu-ABY-027, the same dose to tumor would be achieved with 33.1 MBq. With the specific activity used in the present study, this would require injection of 22-25 µg ^{177}Lu-ABY-027 per mouse. As shown in the present study, this is in a range, where small differences in the injected protein dose have insignificant effect on tumor uptake. A comparison at equal dose to tumor shows that the dose to blood and bone would be very similar for the two constructs, and that ^{177}Lu-ABY-027 would give 2.8-fold and 1.8-fold lower dose to kidney and liver, respectively.

CONCLUSIONS

$Z_{HER2:2891}$-ABD_{035}-DOTA (ABY-027) is a fusion protein having a biodistribution suitable for therapy and showing retained HER2-specific binding. The capacity of specific targeting of HER2-expressing xenografts was shown in vivo. In a murine model, ^{177}Lu-ABY-027 provided an appreciable reduction of renal and hepatic uptake of radioactivity in comparison with alternative approaches. Site-specific conjugation of DOTA provides a uniform conjugate and creates potential for labeling with a broad range of therapeutic radionuclides. The unique cysteine can also be used for site specific coupling of other effector functions.

ACKNOWLEDGMENT

This work was supported by grants from Swedish Research Council (Vetenskapsrådet) and Swedish Cancer Society (Cancerfonden).

REFERENCES

1. Carlsson J. Potential for clinical radionuclide-based imaging and therapy of common cancers expressing EGFR-family receptors. *Tumour Biol*. 2012;33:653-659
2. Buzdar AU, Ibrahim NK, Francis D et al. Significantly higher pathologic complete remission rate after neoadjuvant therapy with trastuzumab, paclitaxel, and epirubicin chemotherapy: Results of a randomized trial in human epidermal growth factor receptor 2-positive operable breast cancer. *J Clin Oncol*. 2005;23:3676-3685.
3. Nahta R, Esteva FJ. Trastuzumab: triumphs and tribulations. *Oncogene* 2007;26:3637-3643.
4. Senter PD. Potent antibody drug conjugates for cancer therapy. *Curr Opin Chem Biol*. 2009;13:235-244.
5. Kassis AI, Adelstein SJ. Radiobiologic principles in radionuclide therapy. *J Nucl Med. 2005*;46(Suppl 1):4S-12S.
6. Goldsmith SJ. Radioimmunotherapy of lymphoma: Bexxar and Zevalin. *Semin Nucl Med*. 2010;40:122-135.
7. Sharkey RM, Goldenberg DM. Perspectives on cancer therapy with radiolabeled monoclonal antibodies. *J Nucl Med*. 2005;46(Suppl 1):115S-27S.
8. Jain M, Venkatraman G, Batra SK. Optimization of radioimmunotherapy of solid tumors: biological impediments and their modulation. *Clin Cancer Res*. 2007; 13:1374-1382.

9. Behr TM, Goldenberg DM, Becker W. Reducing the renal uptake of radiolabeled antibody fragments and peptides for diagnosis and therapy: present status, future prospects and limitations. *Eur J Nucl Med*. 1998;25:201–212.
10. Schmidt MM, Wittrup KD. A modeling analysis of the effects of molecular size and binding affinity on tumor targeting. *Mol Cancer Ther*. 2009;8:2861-2871.
11. Orlova A, Magnusson M, Eriksson TL, et al. Tumor imaging using a picomolar affinity HER2 binding affibody molecule. *Cancer Res*. 2006;66:4339-4348.
12. Nygren P-Å. Alternative binding proteins: Affibody binding proteins developed from a small three-helix bundle scaffold. *FEBS J*. 2008;275:2668-2676.
13. Löfblom J, Feldwisch J, Tolmachev V, Carlsson J, Ståhl S, Frejd FY. Affibody molecules: engineered proteins for therapeutic, diagnostic and biotechnological applications. *FEBS Lett*. 2010;584:2670-2680.
14. Baum RP, Prasad V, Müller D, et al. Molecular imaging of HER2-expressing malignant tumors in breast cancer patients using synthetic 111In- or 68Ga-labeled affibody molecules. *J Nucl Med*. 2010;51:892-897.
15. Orlova A, Tolmachev V, Pehrson R, et al. Synthetic affibody molecules: a novel class of affinity ligands for molecular imaging of HER2-expressing malignant tumors. *Cancer Res*. 2007;67:2178-2182.
16. Fortin MA, Orlova A, Malmström PU, Tolmachev V. Labelling chemistry and characterization of [^{90}Y/^{177}Lu]-DOTA-$Z_{HER2:342}$-3 Affibody molecule, a candidate agent for locoregional treatment of urinary bladder carcinoma. *Int J Mol Med*. 2007;19:285-291.
17. Tolmachev V, Orlova A, Pehrson R, et al. Radionuclide therapy of HER2-positive micro-xenografts using a 177Lu-labeled HER2-specific Affibody molecule. *Cancer Res*. 2007;67:2773-2782.

18. Tolmachev V, Wållberg H, Andersson K, Wennborg A, Lundqvist H, Orlova A. The influence of Bz-DOTA and CHX-A''-DTPA on the biodistribution of ABD-fused anti-HER2 Affibody molecules: implications for (114m)In-mediated targeting therapy. *Eur J Nucl Med Mol Imaging*. 2009;36:1460-1468.
19. Dennis MS, Jin H, Dugger D, et al. Imaging tumors with an albumin-binding Fab, a novel tumor-targeting agent. *Cancer Res*. 2007;67:254-261.
20. Kratz F. Albumin as a drug carrier: Design of prodrugs, drug conjugates and nanoparticles. *J Controlled Release*. 2008;132:171–183.
21. Jonsson A, Dogan J, Herne N, Abrahmsén L, Nygren PA. Engineering of a femtomolar affinity binding protein to human serum albumin. *Protein Eng Des Sel*. 2008;21:515-527.
22. Feldwisch J, Tolmachev V, Lendel C, et al. Design of an optimized scaffold for affibody molecules. *J Mol Biol*. 2010;398:232-247.
23. Sandberg D, Wennborg A, Feldwisch J, et al. First clinical observations of HER2 specific [111In]ABY-025 metastatic detection capability in females with metastatic breast cancer [abstract]. *J Nucl Med*. 2012;53(Suppl.):220.
24. Ahlgren S, Orlova A, Wållberg H, et al. Targeting of HER2-expressing tumors using 111In-ABY-025, a second-generation affibody molecule with a fundamentally reengineered scaffold. *J Nucl Med*. 2010;51:1131-1138.
25. Tolmachev V, Tran TA, Rosik D, Sjöberg A, Abrahmsén L, Orlova A. Tumor targeting using affibody molecules: interplay of affinity, target expression level, and binding site composition. *J Nucl Med*. 2012;53:953-960.
26. Wållberg H, Orlova A. Slow internalization of anti-HER2 synthetic affibody monomer ^{111}In-DOTA-$Z_{HER2:342}$-pep2: implications for development of labeled tracers. *Cancer Biother Radiopharm*. 2008;23:435-442.

27. Smith-Jones PM, Solit DB, Akhurst T, Afroze F, Rosen N, Larson SM. Imaging the pharmacodynamics of HER2 degradation in response to Hsp90 inhibitors. *Nat Biotechnol*. 2004;22:701-706.
28. Adams GP, Shaller CC, Dadachova E, et al. A single treatment of yttrium-90-labeled CHX-A"-C6.5 diabody inhibits the growth of established human tumor xenografts in immunodeficient mice. *Cancer Res*. 2004;64:6200-6206.
29. Zahnd C, Kawe M, Stumpp MT, et al. Efficient tumor targeting with high-affinity designed ankyrin repeat proteins: effects of affinity and molecular size. *Cancer Res*. 2010;70:1595-1605
30. Vaneycken I, Devoogdt N, Van Gassen N, et al. Preclinical screening of anti-HER2 nanobodies for molecular imaging of breast cancer. *FASEB J*. 2011;25:2433-2446
31. Andersen JT, Pehrson R, Tolmachev V, Daba MB, Abrahmsén L, Ekblad C. Extending half-life by indirect targeting of the neonatal Fc receptor (FcRn) using a minimal albumin binding domain. *J Biol Chem*. 2011;286:5234-5241.
32. Garmestani K, Milenic DE, Plascjak PS, Brechbiel MW. A new and convenient method for purification of ^{86}Y using a Sr(II) selective resin and comparison of biodistribution of ^{86}Y and ^{111}In labeled Herceptin. *Nucl Med Biol*. 2002;29:599-606.
33. Hoppmann S, Miao Z, Liu S, et al. Radiolabeled affibody-albumin bioconjugates for HER2-positive cancer targeting. *Bioconjug Chem*. 2011;22:413-421.
34. Lövqvist A, Humm JL, Sheikh A, et al. PET imaging of (86)Y-labeled anti-Lewis Y monoclonal antibodies in a nude mouse model: comparison between (86)Y and (111)In radiolabels. *J Nucl Med*. 2001;42:1281-1287.

Table 1. Comparison of biodistribution of radiolabeled potential affibody-based therapeutics in tumor bearing mice.

	Concentration of radioactivity, %ID/g 48 h pi					
	^{111}In-ABY-027[a]	**^{111}In-CHX-A''-DTPA-ABD-($Z_{HER2:342}$)$_2$[a]**	**^{177}Lu-ABY-027[a]**	**^{177}Lu-CHX-A''-DTPA-ABD-($Z_{HER2:342}$)$_2$[a] (*17*)**	**^{111}In-DOTA-ABD-($Z_{HER2:342}$)$_2$[b] (*18*)**	**^{111}In-DOTA-HSA-($Z_{HER2:342}$)$_n$[a] (*33*)**
Tumor	43±3	22 ±7	17±7	26 ±4	12±3	17 ± 1
Blood	5.9±0.8	4.7±1.0	5.3±0.4	5.5±0.8	4.6±1.0	3.0±0.9
Lung	4.5±0.4	3.4±0.7	3.5±0.5	3.5±0.5	3.3±0.6	2.6±0.6
Liver	7.0±0.9	6±2	3.0±0.7	5.7±0.6	5.2±0.8	14±3
Spleen	5.4±0.8	3.2±0.9	2.9±0.5	3.8±0.4	5±2	9±1
Kidney	6.0±0.6	17±3	3.9±0.6	15.9±0.8	18±2	5.7±0.9
Muscle	1.0±0.2	0.7±0.2	1.4±0.4	1.0±0.3	0.7±0.2	1.0 ±0.3
Bone	1.54±0.08	1.0±0.3	1.2±0.4	1.8±0.6	1.7±0.6	3.33 ±0.05

a SKOV-3 ovarian carcinoma xenografts, high HER2-expression

b LS174T colorectal carcinoma xenografts, low HER2-expression

Table 2. Biodistribution of ^{177}Lu-ABY-027 (injected dose 10 μg) in Balb/C nu/nu mice bearing HER2-expressing SKOV-3 xenografts.

	Concentration of radioactivity, %ID/g					
	4 h	**1 d**	**2 d**	**3 d**	**7 d**	**14 d**
Tumor	1.1±0.5	8±1	17±7	15±3	7±2	1.3±0.2
Blood	5±1	8±2	5.3±0.4	3.4±0.4	0.39±0.05	0.020±0.003
Heart	1.3±0.3	2.7±0.5	2.4±0.3	1.9±0.2	0.7±0.2	0.21±0.04
Lung	2.1±0.4	4.1±0.7	3.5±0.5	2.4±0.2	0.6±0.1	0.13±0.03
Liver	1.0±0.2	2.8±0.8	3.0±0.7	2.5±0.3	1.2±0.2	0.52±0.03
Spleen	0.6±0.1	2.3±0.5	2.9±0.5	2.5±0.6	1.9±0.6	1.0±0.6
Pancreas	0.45±0.06	1.3±0.2	1.0±0.2	0.8±0.2	0.27±0.05	0.10±0.03
Stomach	0.41±0.05	1.5±0.2	1.5±0.6	0.9±0.1	0.25±0.04	0.08±0.01
Kidney	2.6±0.4	4.3±0.8	3.9±0.6	2.98±0.09	1.3±0.2	0.39±0.06
Muscle	1.4±0.4	1.3±0.2	1.4±0.4	0.9±0.2	0.36±0.08	0.09±0.03
Bone	0.7±0.2	1.3±0.2	1.2±0.4	1.1±0.2	0.5±0.3	0.5±0.2
Intestines*	0.9±0.3	1.9±0.5	3±2	1.3±0.4	0.40±0.07	0.10±0.02
Carcass*	58±15	46±2	39±2	32±2	12±1	6.1±0.4

Data are presented as an average of % ID/g±SD, n=4.

*Data for intestines with content and carcass are presented as %ID per whole sample.

Table 3. Dosimetry of ^{177}Lu-ABY-027 in mice in comparison with ^{177}Lu-CHX-A''-DTPA-ABD-$(Z_{HER2:342})_2$ (*17*).

Organ	**^{177}Lu-ABY-027**	**^{177}Lu-CHX-A''-DTPA-ABD-$(Z_{HER2:342})_2$**
	Gy/MBq	
Blood	0.42±0.04	0.51±0.3
Heart	0.21±0.01	0.25±0.02
Lung	0.27±0.02	0.33±0.01
Liver	0.28±0.01	0.76±0.03
Spleen	0.32±0.04	0.53±0.4
Pancreas	0.091±0.008	0.12±0.01
Stomach	0.10±0.01	0.097±0.003
Intestine	0.10±0.01	0.11±0.005
Kidney	0.35±0.02	1.49±0.07
Tumor	1.37±0.22	2.1±0.2
Muscle	0.11±0.01	0.09±0.001
Bone	0.13±0.02	0.21±0.05

Data are presented as an average Gy/MBq±SD, n=4.

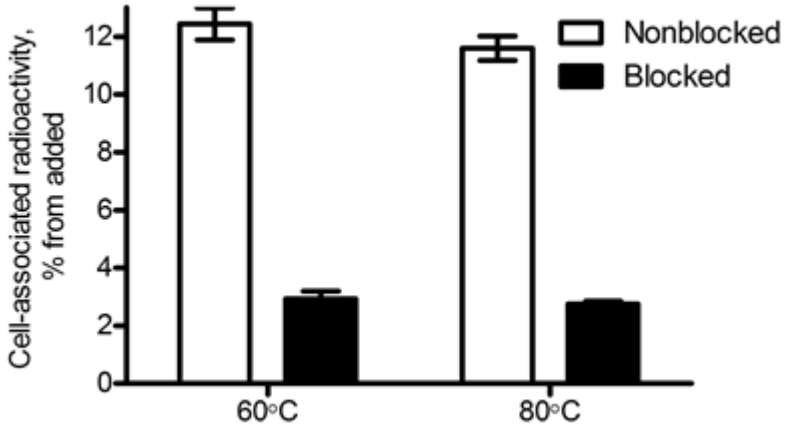

Figure 1. In vitro specificity test for ^{177}Lu-ABY-027 labeled at 60°C and 80°C on SKOV-3 cells (average of 3±SD).

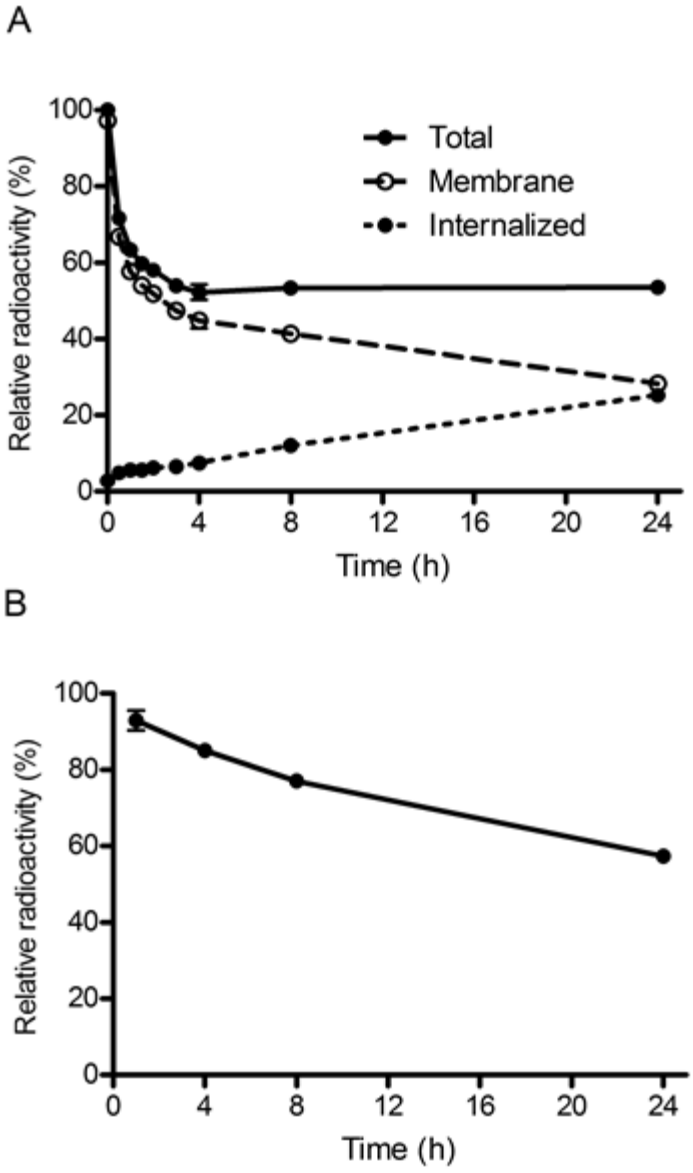

Figure 2. **A**. Cellular processing of ^{177}Lu-ABY-027 in SKOV-3 cells after interrupted incubation (average of three samples±SD). In each sample the radioactivity was normalized by the cell-associated radioactivity at the time of interruption. **B**. Size-exclusion analysis of incubation media after interrupted incubation of ^{177}Lu-ABY-027 with SKOV-3 cells (average of 2±SD).

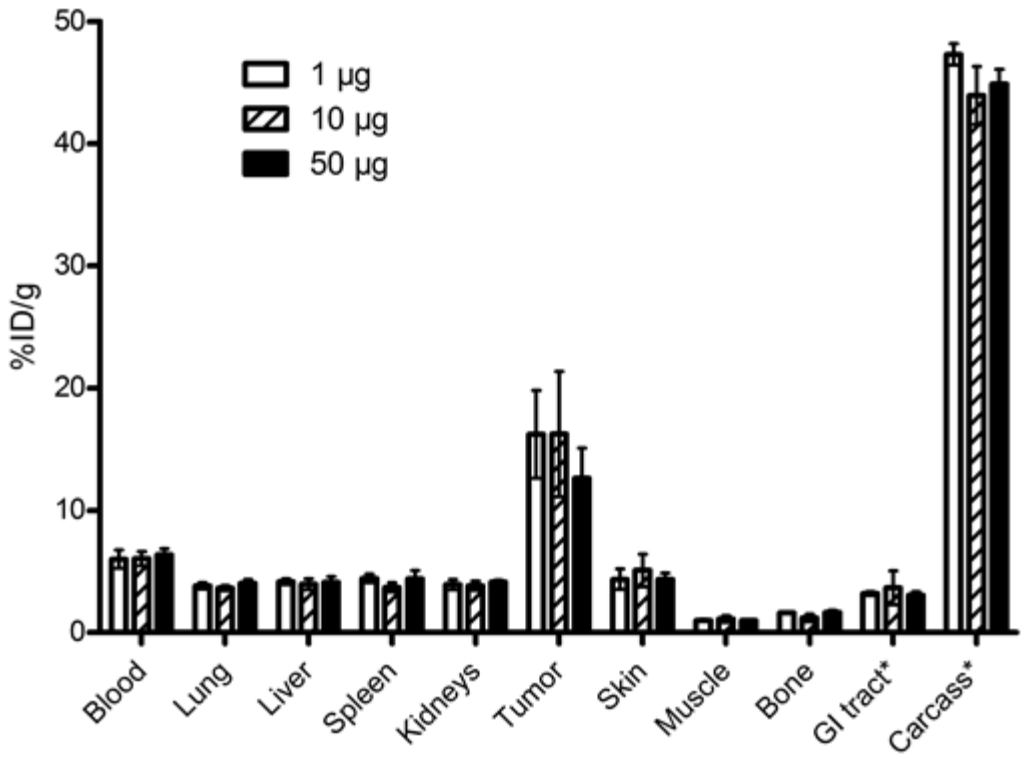

Figure 3. Uptake of radioactivity 48 h after injection of 1, 10 or 50 µg ^{177}Lu-ABY-027 in SKOV-3 xenografted mice (average of 4-6, %ID/g±SD). *For gastrointestinal tract (with content) and carcass data are presented as %ID per whole sample.

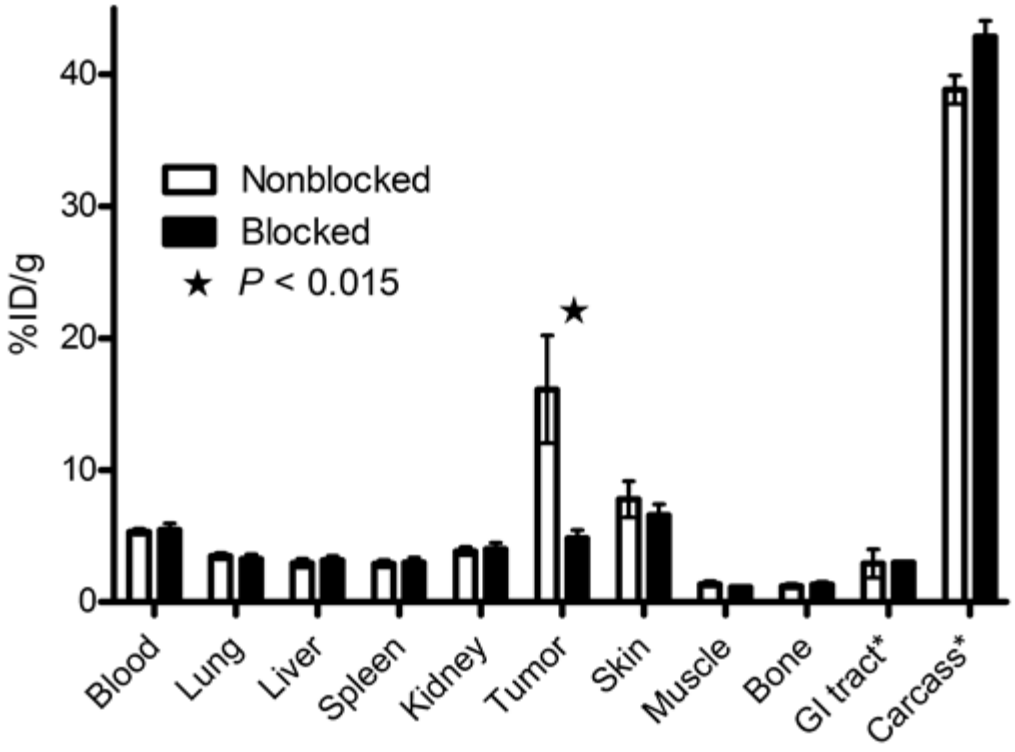

Figure 4. *In vivo* binding specificity of ^{177}Lu-ABY-027, 48 h pi ((average of 4, %ID/g±SD)). The blocked group was pre-injected with 1 mg of non-labeled ABY-027. *For gastrointestinal tract (with content) and carcass data are presented as %ID per whole sample.